

## The Divalent Metal Ion in the Active Site of Uteroferrin Modulates Substrate Binding and Catalysis

Nataša Mitić,<sup>†</sup> Kieran S. Hadler,<sup>†</sup> Lawrence R. Gahan,<sup>†</sup> Alvan C. Hengge,<sup>\*,‡</sup> and Gerhard Schenk<sup>\*,†</sup>

School of Chemistry and Molecular Biosciences, The University of Queensland, St. Lucia, Queensland, 4072, Australia and Department of Chemistry and Biochemistry, Utah State University, Logan, Utah 84322-0300

Received December 15, 2009; E-mail: schenk@uq.edu.au; alvan.hengge@usu.edu

**Abstract:** The purple acid phosphatases (PAP) are binuclear metallohydrolases that catalyze the hydrolysis of a broad range of phosphomonoester substrates. The mode of substrate binding during catalysis and the identity of the nucleophile is subject to debate. Here, we used native  $\text{Fe}^{3+}$ – $\text{Fe}^{2+}$  pig PAP (uteroferrin; Uf) and its  $\text{Fe}^{3+}$ – $\text{Mn}^{2+}$  derivative to investigate the effect of metal ion substitution on the mechanism of catalysis. Replacement of the  $\text{Fe}^{2+}$  by  $\text{Mn}^{2+}$  lowers the reactivity of Uf. However, using stopped-flow measurements it could be shown that this replacement facilitates approximately a ten-fold faster reaction between both substrate and inorganic phosphate with the chromophoric  $\text{Fe}^{3+}$  site. These data also indicate that in both metal forms of Uf, phenyl phosphate hydrolysis occurs faster than formation of a  $\mu$ -1,3 phosphate complex. The slower rate of interaction between substrate and the  $\text{Fe}^{3+}$  site relative to catalysis suggests that the substrate is hydrolyzed while coordinated only to the divalent metal ion. The likely nucleophile is a water molecule in the second coordination sphere, activated by a hydroxide terminally coordinated to  $\text{Fe}^{3+}$ . The faster rates of interaction with the  $\text{Fe}^{3+}$  site in the  $\text{Fe}^{3+}$ – $\text{Mn}^{2+}$  derivative than the native  $\text{Fe}^{3+}$ – $\text{Fe}^{2+}$  form are likely mediated via a hydrogen bond network connecting the first and second coordination spheres, and illustrate how the selection of metal ions may be important in fine-tuning the function of this enzyme.

### 1. Introduction

Purple acid phosphatases (PAPs) belong to the family of binuclear metallohydrolases and hydrolyze mono- and some diester substrates at acidic to neutral pH.<sup>1–4</sup> PAPs require heterovalent  $\text{Fe}^{3+}$ – $\text{M}^{2+}$  centers ( $M = \text{Fe}, \text{Zn}, \text{Mn}$ ) for catalysis, and their characteristic purple color is due to a charge transfer (CT) interaction between a conserved tyrosine ligand and the  $\text{Fe}^{3+}$  in the active site. The biological functions of PAPs are diverse and include phosphate acquisition and reactive oxygen species metabolism in plants and bacterial killing and bone resorption in animals.<sup>3,5,6</sup>

In the proposed mechanistic model of the PAP-catalyzed reaction the substrate initially associates with the enzyme forming a catalytically noncompetent complex.<sup>3,7–11</sup> Subsequently, rearrangements within the active site lead to the formation of a Michaelis complex where the oxygen atom of the phosphate group of the substrate is monodentately coordi-

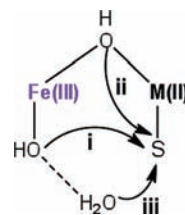


**Figure 1.** Proposed nucleophilic hydroxide molecules for PAP-catalyzed hydrolysis are positioned (i) terminal to  $\text{Fe}^{3+}$ ; (ii) bridging the two metal ions; or (iii) residing in the second coordination sphere.

nated to the divalent metal ion. A number of aspects of the subsequent reaction sequence are uncertain. While the next step in the catalytic cycle involves a nucleophilic attack by a hydroxide, the identity of the nucleophile has been proposed to depend on the type of substrate and the metal ion composition in the active site.<sup>11</sup> The nucleophilic hydroxide has been proposed to be (i) terminally bound to  $\text{Fe}^{3+}$ ; (ii) bridging the two metal ions; or (iii) residing in the second coordination sphere (Figure 1).<sup>3,4,7–11</sup> The mode of substrate binding in the Michaelis complex is also uncertain. Both  $\text{M}^{2+}$  monodentate and  $\mu$ -1,3 bidentate coordination have been suggested based on a range of crystallographic, spectroscopic, and kinetic studies.<sup>3,4,7–13</sup>

The nucleophile used in the reaction and the orientation of the substrate are likely to be associated; i.e., the identity of the

<sup>†</sup> The University of Queensland.

<sup>‡</sup> Utah State University.

- (1) Sträter, N.; Lipscomb, W. N.; Klabunde, T.; Krebs, B. *Angew. Chem., Int. Ed. Engl.* **1996**, *35*, 2025–2055.
- (2) Wilcox, D. E. *Chem. Rev.* **1996**, *96*, 2435–2458.
- (3) Mitić, N.; Smith, S. J.; Neves, A.; Guddat, L. W.; Gahan, L. R.; Schenk, G. *Chem. Rev.* **2006**, *106*, 3338–3363.
- (4) Cox, R. S.; Schenk, G.; Mitić, N.; Gahan, L. R.; Hengge, A. C. *J. Am. Chem. Soc.* **2007**, *129*, 9550–9551.
- (5) Oddie, G. W.; Schenk, G.; Angel, N. Z.; Walsh, N.; Guddat, L. W.; de Jersey, J.; Cassady, A. I.; Hamilton, S. E.; Hume, D. A. *Bone* **2000**, *27*, 575–584.
- (6) Bozzo, G. G.; Raghothama, K. G.; Plaxton, W. C. *Biochem. J.* **2004**, *377*, 419–428.

- (7) Smoukov, S. K.; Quaroni, L.; Wang, X.; Doan, P. E.; Hoffman, B. M.; Que, L., Jr. *J. Am. Chem. Soc.* **2002**, *124*, 2595–2603.
- (8) Merx, M.; Pinkse, M. W. H.; Averill, B. A. *Biochemistry* **1999**, *38*, 9914–9925.

nucleophile in the PAP-catalyzed reaction depends upon the mode of substrate binding. For instance, for a metal ion-bridging nucleophile the optimal alignment with the substrate is reached when the latter binds in  $\mu$ -1,3 bidentate coordination to the active site.<sup>12–14</sup> If the substrate reacts while bound only to the divalent metal ion, a hydroxide either terminally bound to  $\text{Fe}^{3+}$  or in the second coordination sphere is a more likely candidate as a nucleophile (Figure 1).

To probe the mode of substrate binding to PAP, and the effect of the metal ion composition thereof, we have used the PAP enzyme from pig (also known as uteroferrin; Uf) and employed stopped-flow measurements to monitor the CT interaction with inorganic phosphate and with phenyl phosphate, in two different metal ion derivatives, the native  $\text{Fe}^{3+}$ – $\text{Fe}^{2+}$  and the  $\text{Fe}^{3+}$ – $\text{Mn}^{2+}$  forms.

## 2. Materials and Methods

**Materials.** All chemicals used were of analytical grade and were purchased from Sigma unless otherwise stated.

**Enzyme Purification.** Pig PAP (uteroferrin; Uf) was isolated from the uterine fluid as described previously.<sup>15</sup> In brief, Uf was extracted from the uterine fluid of a pregnant sow; an initial ion-exchange chromatography step using CM-cellulose resin was followed by gel filtration on a Sephadex G-75 column. Purified Uf was stored at  $-20\text{ }^\circ\text{C}$  in 100 mM acetate buffer at pH 4.9 until further use. The protein concentration was determined by measuring the absorbance at 280 nm using the specific extinction of 1.41 for a 1 mg/mL solution (28.6  $\mu\text{M}$ ) of Uf.

**Metal Ion Replacement.** To replace  $\text{Fe}^{2+}$  in the active site of Uf by  $\text{Mn}^{2+}$  500  $\mu\text{L}$  of the enzyme (7 mg; 0.1 M acetate buffer, pH 4.9) were mixed with 1 mL of 30 mM 1,10-phenanthroline (in 0.1 M acetate buffer, pH 4.9) and 500  $\mu\text{L}$  of 100 mM sodium dithionite (freshly prepared in 0.1 M acetate buffer, pH 4.9 immediately prior to use) and incubated at room temperature for 1 min. Subsequently, the mixture was applied to a Bio-Rad Econo-Pac 10DG column (preequilibrated with 0.1 M acetate buffer, pH 4.9). The metal ion content and the activity of the half apo enzyme was determined by atomic absorption spectroscopy (AAS) and a standard activity assay (see below), respectively. For various samples of half apo Uf the iron content varied between 0.89 and 1.06 per active site, with only trace amounts of Zn and Cu detectable. The residual activity never reached values higher than 8 U/mg (less than 3% of the fully active holoenzyme).

To the half apo enzyme 100 equiv of  $\text{Mn}^{2+}$  ( $\text{MnSO}_4$ ) were added, and the activity was monitored until maximum activity was reached. The excess of  $\text{Mn}^{2+}$  was then removed by dialysis, and the content of bound  $\text{Mn}^{2+}$  measured by AAS ( $0.87 \pm 0.05$ ).

**Activity Assay.** A standard continuous assay was used to determine steady-state kinetic constants for Uf with phenyl phosphate (PP) or *para*-nitrophenol phosphate (pNPP) as the

substrate as described elsewhere.<sup>16</sup> Assays were carried out at pH 4.9 using 100 mM acetate buffer. Product formation (P or pNPP) was monitored at 278 and 390 nm, respectively, using appropriate extinction coefficients ( $770\text{ M}^{-1}\text{ cm}^{-1}$  and  $342.9\text{ M}^{-1}\text{ cm}^{-1}$ ).<sup>11,16</sup> Substrate concentrations ranged from  $\sim 0.2 \times K_m$  to  $\sim 8 \times K_m$ . Assay mixtures were incubated at  $25\text{ }^\circ\text{C}$  for 5 min prior to the addition of enzyme (20 nM). Data displayed saturation type behavior (Michaelis–Menten behavior), and kinetic parameters were determined by fitting to eq 1 using WinCurveFit (Kevin Raner software):

$$v = \frac{V_{\max} \times [S]}{K_m + [S]} \quad (1)$$

Here,  $v$  is the initial rate,  $[S]$  is the substrate concentration,  $V_{\max}$  is  $k_{\text{cat}}$  multiplied by the amount of enzyme present, and  $K_m$  is the Michaelis constant.

**pH Dependence Studies.** Activity assays with pNPP and PP as substrate were carried out at 11 pH values between pH 3 and pH 7.5 using 100 mM glycine, acetate, or 2-morpholinoethanesulfonic acid buffers, respectively. The  $k_{\text{cat}}$  and  $k_{\text{cat}}/K_m$  versus pH data were fit to the following equations using WinCurveFit:

$$k_{\text{cat}} = \frac{(k_{\text{cat}})^{\max}}{(1 + [\text{H}]/K_{\text{es}1} + K_{\text{es}2}/[\text{H}])} \quad (2)$$

$$k_{\text{cat}}/K_m = \frac{(k_{\text{cat}}/K_m)^{\max}}{(1 + [\text{H}]/K_{\text{e}1} + K_{\text{e}2}/[\text{H}])} \quad (3)$$

$K_{\text{e}i}$  and  $K_{\text{e}si}$  ( $i = 1, 2$ ) are apparent acid dissociation constants of the enzyme and/or substrate ( $K_{\text{e}i}$ ) and the enzyme–substrate complex ( $K_{\text{e}si}$ ), and  $[\text{H}]$  is the proton concentration.<sup>17,18</sup> For FeMn Uf only the alkaline limb is resolved (i.e.,  $K_{\text{e}1} \gg K_{\text{e}2}$ ); thus data were fit to the following equation.

$$k_{\text{cat}}/K_m = \frac{(k_{\text{cat}}/K_m)^{\max}}{(1 + K_{\text{e}2}/[\text{H}])} \quad (4)$$

**Stopped-Flow Measurements.** The reactions of native Uf and  $\text{Fe}^{3+}$ – $\text{Mn}^{2+}$  Uf with the substrate PP were monitored at 620 nm,  $25\text{ }^\circ\text{C}$ ,  $I = 0.1\text{ M}$  (NaCl), using an Applied Photophysics SX-18MV stopped-flow spectrophotometer. After mixing the enzyme concentration was 45  $\mu\text{M}$  and substrate concentrations ranged from 3.75 mM to 50 mM. Similar to reactions previously recorded with phosphate as substrate,<sup>19,20</sup> the time course of the absorbance change is described by a uniphase first-order fit; corresponding  $k_{\text{obs}}$  values were obtained using software provided by Applied Photophysics. In general, average  $k_{\text{obs}}$  values were obtained from five consecutive measurements.

For the analysis of the data a mechanistic model initially proposed by Sykes and co-worker and recently refined by Hadler et al. was employed (Scheme 1; see text for details).<sup>19,21</sup>

For this scheme an equation of the type

(9) Schenk, G.; Gahan, L. R.; Carrington, L. E.; Mitić, N.; Valizadeh, M.; Hamilton, S. E.; de Jersey, J.; Guddat, L. W. *Proc. Natl. Acad. Sci. U.S.A.* **2005**, *102*, 273–278.

(10) Mitić, N.; Noble, C. J.; Gahan, L. R.; Hanson, G. R.; Schenk, G. *J. Am. Chem. Soc.* **2009**, *131*, 8173–8179.

(11) Smith, S. J.; Casellato, A.; Hadler, K. S.; Mitić, N.; Riley, M. J.; Bortoluzzi, A. J.; Szpoganicz, B.; Schenk, G.; Neves, A.; Gahan, L. R. *J. Biol. Inorg. Chem.* **2007**, *12*, 1207–1220.

(12) Yang, Y. S.; McCormick, J. M.; Solomon, E. I. *J. Am. Chem. Soc.* **1997**, *119*, 11832–11842.

(13) Wang, X.; Ho, R. Y. N.; Whiting, A. K.; Que, L., Jr. *J. Am. Chem. Soc.* **1999**, *121*, 9235–9236.

(14) Schenk, G.; Elliott, T. W.; Leung, E.; Carrington, L. E.; Mitić, N.; Gahan, L. R.; Guddat, L. W. *BMC Struct. Biol.* **2008**, *8*, 6.

(15) Campbell, H. D.; Dionysius, D. A.; Keough, D. T.; Wilson, B. E.; de Jersey, J.; Zerner, B. *Biochem. Biophys. Res. Commun.* **1978**, *82*, 615–620.

(16) Mitić, N.; Valizadeh, M.; Leung, E. W. W.; de Jersey, J.; Hamilton, S.; Hume, D. A.; Cassidy, A. I.; Schenk, G. *Arch. Biochem. Biophys.* **2005**, *439*, 154–164.

(17) Cleland, W. W. *Adv. Enzymol. Relat. Areas Mol. Biol.* **1977**, *45*, 273–387.

(18) Segel, I. H. *Enzyme kinetics: behavior and analysis of rapid equilibrium and steady state enzyme systems*; Wiley: New York, 1975.

(19) Twitchett, M. B.; Schenk, G.; Aquino, M. A. S.; Yiu, D. T. Y.; Lau, T. C.; Sykes, A. G. *Inorg. Chem.* **2002**, *41*, 5787–5794.

(20) Aquino, M. A. S.; Lim, J. S.; Sykes, A. G. *J. Chem. Soc., Dalton Trans.* **1994**, 429–436.

(21) Hadler, K.; Mitić, N.; Ely, F.; Hanson, G. R.; Gahan, L. R.; Larrabee, J. A.; Ollis, D. L.; Schenk, G. *J. Am. Chem. Soc.* **2009**, *131*, 11900–11908.





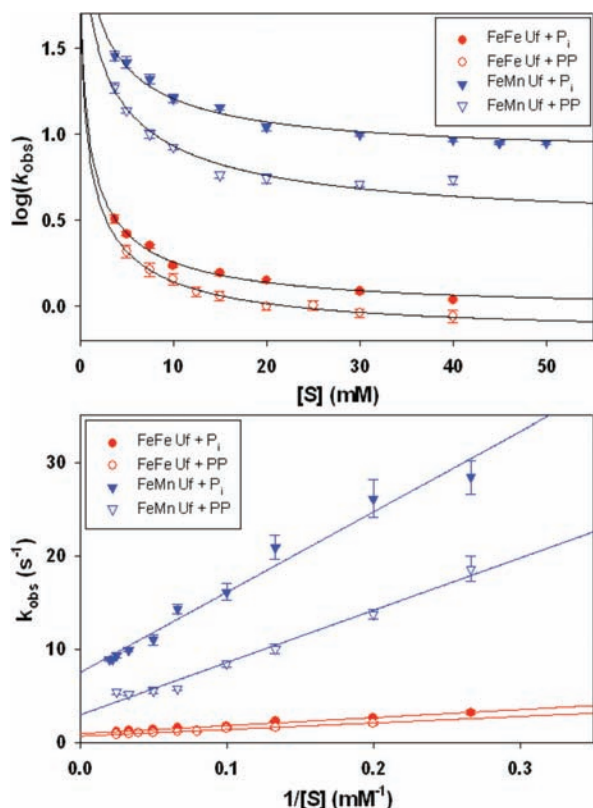


**Figure 3.** First-order rate constants ( $k_{\text{obs}}$ ;  $\text{s}^{-1}$ ) for FeFe Uf (red) and FeMn Uf (blue) at pH 4.9, 25 °C,  $I = 0.1$  M (NaCl). Substrate concentrations ranged from 3.5 to 50 mM. Data for  $\text{P}_i$  were reproduced from ref 19.

assigned to the deprotonation of the metal ion-bridging  $\text{H}_2\text{O}$ .<sup>11</sup> The assignment of  $\text{p}K_{\text{es1}}$  may depend on the metal ion composition. For native  $\text{Fe}^{3+}\text{--Fe}^{2+}$  Uf the likely protonation equilibrium corresponding for  $\text{p}K_{\text{es1}}$  is the terminal  $\text{Fe}^{3+}$ -bound  $\text{H}_2\text{O}/\text{OH}^-$ ,<sup>11</sup> while for the  $\text{Fe}^{3+}\text{--Ni}^{2+}$  derivative  $\text{p}K_{\text{es1}}$  has been assigned to the deprotonation of the  $\mu$ -hydroxide.<sup>26</sup> The latter is likely to be the case for FeMn Uf based on the similarity of its  $\text{p}K_{\text{es1}}$  to the corresponding constant in FeMn sweet potato PAP.<sup>9,10</sup> The assignments of  $\text{p}K_{\text{es1}}$  to two different equilibria (i.e., terminal  $\text{Fe}^{3+}$ -bound  $\text{H}_2\text{O}/\text{OH}^-$  and  $\mu\text{--OH}^-/\mu\text{--O}^{2-}$ ) were also interpreted in terms of different nucleophiles operational in these two PAPs, i.e. a terminal hydroxide in the diiron enzyme and a bridging (hydr)oxide in the FeNi and FeMn systems.<sup>9–11,26</sup> Thus, the comparative monitoring of CT perturbations by stopped-flow spectroscopy between the FeFe and FeMn forms of Uf may provide insights into alternative modes of substrate binding during hydrolysis.

The rates of perturbation ( $k_{\text{obs}}$ ) observed for both the native di-iron and the FeMn Uf (Figure 3) decrease with increasing [PP] or  $[\text{P}_i]$ , a trend that has also been observed for a binuclear glycerophosphodiesterase from *Enterobacter aerogenes* (GpdQ).<sup>21</sup> The model employed to analyze/fit the data is described in detail elsewhere.<sup>19,21</sup> In brief, rapid initial binding of the substrate in a catalytically noncompetent mode (ES in Scheme 1) is followed by subsequent rearrangements that lead to a direct coordination of the substrate to the divalent metal

**Table 2.** Fit of  $k_{\text{obs}}$  vs  $[\text{S}]$  Data Using an Equation Derived for the Model Described in Ref 21 (See Materials and Methods for Details)

Uf form	Substrate	$k_{\text{on}}/K_i$ ( $\text{mM s}^{-1}$ )	$k_{\text{off}}$ ( $\text{s}^{-1}$ )
FeFe <sup>7</sup>	$\text{P}_i$	8.6 (4)	0.94 (5)
FeFe	PP	7.0 (2)	0.69 (2)
FeMn <sup>7</sup>	$\text{P}_i$	90 (5)	7.5 (6)
FeMn	PP	60 (3)	3.0 (4)

ion (ES' in Scheme 1).<sup>19,21</sup> Binding of a second substrate molecule prevents the formation of a catalytically competent Michaelis complex, thus leading to the observed inhibition at high  $[\text{S}]$  (SES' in Scheme 1).<sup>19,21</sup> In this scheme  $k_{\text{on}}$  and  $k_{\text{off}}$  represent the rate constants for the closure and opening, respectively, of the  $\mu$ -1,3 phosphate bridge. This bridge closure (i) can take place concomitantly with hydrolysis if an  $\text{Fe}^{3+}$ -bound terminal hydroxide acts as the nucleophile (leading to the formation of an EP' complex) or (ii) precedes hydrolysis if the metal ion-bridging hydroxide is the nucleophile (i.e., the formation of an ES'' complex precedes the formation of an EP complex).  $K_{\text{ass1}}$ ,  $K_{\text{ass2}}$ , and  $K_i$  are equilibrium constants representing binding of the substrate ( $K_{\text{ass1}}$  and  $K_{\text{ass2}}$ ) and binding of an inhibitory second substrate molecule ( $K_i$ ), respectively. Scheme 1 predicts mixed inhibition by phosphate and substrate inhibition at high  $[\text{S}]$ . Both of these phenomena have been documented in the closely related bovine spleen PAP.<sup>27</sup>

The data in Figure 3 cannot unambiguously be fit using eq 5; however,  $k_{\text{off}}$  and the ratio  $k_{\text{on}}/K_i$  can be estimated accurately because at high substrate concentrations eq 5 can be simplified to eq 6, as described in Hadler et al.<sup>21</sup> Hence, a plot of  $k_{\text{obs}}$  vs  $[\text{S}]^{-1}$  is linear with  $k_{\text{off}}$  as the intercept and the ratio  $k_{\text{on}}/K_i$  as the slope. These parameters are summarized in Table 2. While  $K_i$  cannot be determined, some bounds can be estimated. The  $K_M$  values of aryl phosphate substrates are  $\sim 1$  mM.<sup>28</sup> Binding of the inhibitory second molecule is expected to be significantly weaker than the first; this ratio has been estimated to be  $\sim 1000$  for *p*NPP and  $\sim 40$  for naphthyl phosphate.<sup>27</sup> This leads to a range for  $K_i$  of between 0.025 and 0.001  $\text{mM}^{-1}$ . This yields estimated bounds for  $k_{\text{on}}$  of between 1.5  $\text{s}^{-1}$  and 0.06  $\text{s}^{-1}$  for PP with the FeMn enzyme and similar values for  $\text{P}_i$ . This analysis places  $k_{\text{on}}$  in a range that is considerably smaller than the  $k_{\text{cat}}$  for PP (Table 1). The same conclusion holds for the FeFe form, where the estimates for  $k_{\text{on}}$  will be approximately an order of magnitude smaller (i.e.,  $\ll 1$   $\text{s}^{-1}$ ).

The  $k_{\text{on}}$  and  $k_{\text{off}}$  rates are higher in the Mn derivative than in the native enzyme, independent of the substrate. It is interesting to note that the water exchange rates of  $[\text{Fe}(\text{H}_2\text{O})_6]^{2+}$  and  $[\text{Mn}(\text{H}_2\text{O})_6]^{2+}$  follow the same trend, with the  $\text{Mn}^{2+}$  complex being approximately an order of magnitude faster.<sup>29</sup>

The mechanistic relevance of the  $k_{\text{on}}$  values emerges from their comparison with catalytic turnover numbers for PP in Table 1. For both forms of Uf ( $\text{Fe}^{3+}\text{--Fe}^{2+}$  and  $\text{Fe}^{3+}\text{--Mn}^{2+}$ ), the estimates of  $k_{\text{on}}$  with PP are considerably slower than  $k_{\text{cat}}$  (195  $\text{s}^{-1}$  and 33  $\text{s}^{-1}$ , respectively). This indicates that hydrolysis precedes formation of the  $\mu$ -1,3 phosphate bridge and the accompanying CT perturbation. The observation that hydrolysis takes place without perturbing the  $\text{Fe}^{3+}$  site (i.e., hydrolysis

(26) Schenk, G.; Peralta, R. A.; Batista, S. C.; Bortoluzzi, A. J.; Szpoganicz, B.; Dick, A. K.; Herrald, P.; Hanson, G. R.; Szilagyi, R. K.; Riley, M. J.; Gahan, L. R.; Neves, A. J. *Biol. Inorg. Chem.* **2008**, *13*, 139–155.

(27) Vincent, J. B.; Crowder, M. W.; Averill, B. A. *Biochemistry* **1992**, *31*, 3033–3037.

(28) Valizadeh, M.; Schenk, G.; Nash, K.; Oddie, G. W.; Guddat, L. W.; Hume, D. A.; de Jersey, J.; Burke, T. R., Jr.; Hamilton, S. *Arch. Biochem. Biophys.* **2004**, *424*, 154–162.

(29) Helm, M.; Merbach, A. E. *Coord. Chem. Rev.* **1999**, *187*, 151–181.

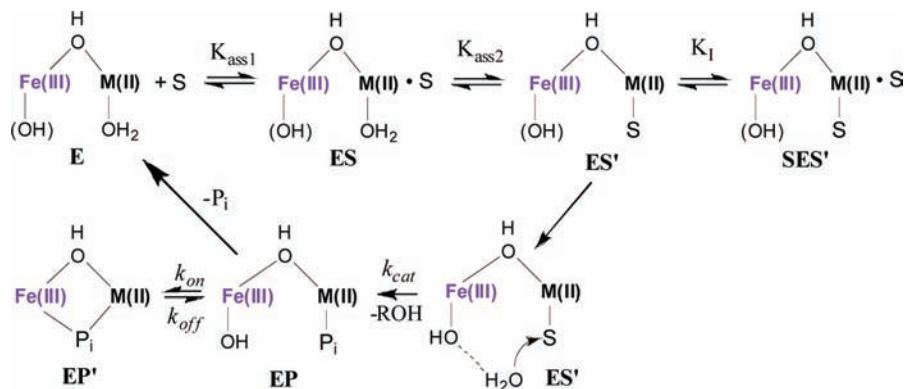
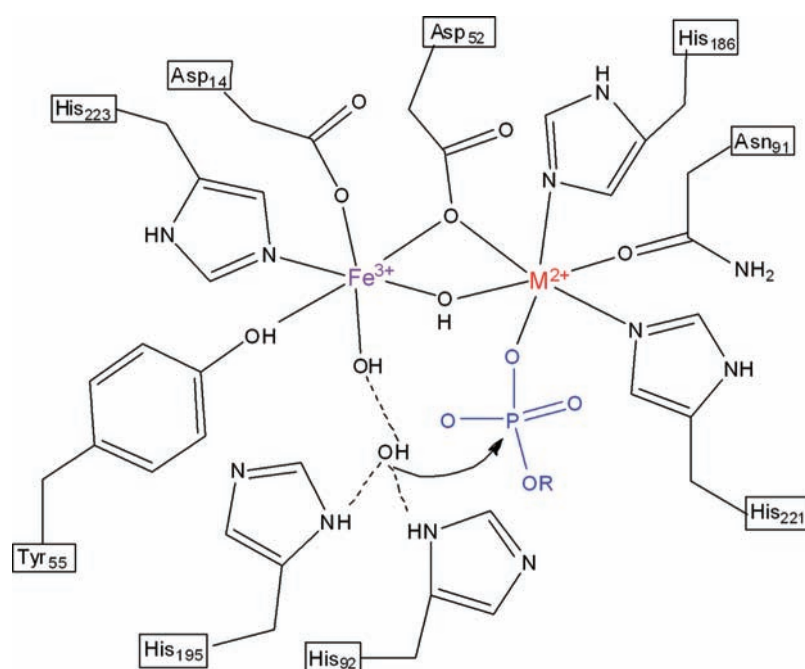


**Figure 4.** Depiction of a mechanism for PAP-catalyzed substrate hydrolysis consistent with the stopped-flow kinetic data.  $K_{\text{ass}1}$  and  $K_{\text{ass}2}$  represent formation of first a noncompetent complex and then an ES complex in which substrate coordinates to the divalent metal ion. Binding of a second, inhibitory substrate molecule occurs with association constant  $K_I$ . Hydrolysis ( $k_{\text{cat}}$ ) occurs from attack by a second-sphere nucleophilic water (see text for additional discussion). Available crystal structures show the presence of several such waters in the outer coordination sphere of the metal center. The nucleophilic water is shown in ES' in the lower part of the figure but omitted from the upper structures for clarity.

**Scheme 2.** Schematic Representation of the Nucleophilic Attack by a Second Coordination Sphere Water Molecule on the Phosphorus Atom of the Substrate



precedes bridge closure; see above and Scheme 1) is difficult to reconcile with a mechanism that requires an  $\text{Fe}^{3+}$ -bound nucleophile. A more plausible reaction sequence thus invokes a nucleophilic water in the second coordination sphere that is deprotonated (i) by the hydroxide terminally coordinated to the  $\text{Fe}^{3+}$  as initially proposed by Averill et al. (ES' in Figure 4)<sup>8</sup> and assisted by hydrogen bonding interactions with conserved histidine residues in the substrate binding pocket (i.e., His92 and His195 in Scheme 2<sup>1,3,9,14,24</sup>). Since PP hydrolysis is more rapid than the rate of CT perturbation, it is likely that only  $\text{P}_i$  binding to the  $\text{Fe}^{3+}$  is observed experimentally, consistent with the similar  $k_{\text{on}}$  rates measured with  $\text{P}_i$  and PP (Table 2). The observed moderate rate differences are ascribed to structural variations in the active site of Uf induced via different hydrogen bond interactions between the enzyme and the respective substrate (i.e.,  $\text{P}_i$  and PP). Thus, the observed on and off rates

are virtually substrate-dependent, representing predominantly a posthydrolysis equilibrium of the enzyme– $\text{P}_i$  complex.

## Conclusion

In conclusion, comparisons of the catalytic parameters with the CT perturbations in two metal ion derivatives of Uf have demonstrated that perturbations to the CT complex occur on a significantly slower time scale than catalysis. The refined reaction model that emerges from the presented work involves a rapid initial binding of the monoester substrate to the enzyme, forming a catalytically noncompetent ES complex (Figure 4). In the next phase of the catalytic cycle the substrate interacts only with the divalent metal ion (ES' complex in Figure 4) and hydrolysis is initiated by a second coordination sphere nucleophilic water that is likely to be activated (i) by a hydroxide that is terminally coordinated to the  $\text{Fe}^{3+}$  and (ii) possibly also by amino acid side chains that line the substrate binding pocket

(e.g., two conserved histidine residues as shown in Scheme 2). Following hydrolysis the  $M^{2+}$ -bound phosphate group (EP complex; Figure 4) is released and replaced by a water molecule, regenerating the active site for the next catalytic cycle. Although both  $k_{on}$  and  $k_{off}$  differ by approximately an order of magnitude depending on the divalent metal ion (Table 2) these differences follow the trend observed for water exchange rates (i.e.,  $Mn^{2+}$  is more rapid than  $Fe^{2+}$ ) and are thus unlikely to be of mechanistic relevance. Hence, irrespective of the identity of the divalent metal ion, Uf is likely to employ a conserved mechanistic strategy whereby the  $M^{2+}$  anchors the substrate monodentately in the active site and the  $Fe^{3+}$  is essential to activate a nucleophile in the second coordination sphere. The formation of the EP' complex in Figure 4 represents thus only

a post- or noncatalytic step describing the interaction between inorganic phosphate and the chromophoric metal ion in the active site.

**Acknowledgment.** This manuscript is dedicated to the memory of Prof. A. G. Sykes. G.S., L.G., and A.H. wish to thank the ARC (DP0986292) and NIH (GM47297) for funding. We are grateful to Prof. W. W. Cleland for helpful comments.

**Note Added after ASAP Publication.** In the version published May 3, 2010, there were errors in the 3rd, 4th and 8th paragraphs of the Materials and Methods section and in the 1st paragraph of the Results and Discussion section. Figure 2 was also replaced. The corrected version published May 4, 2010.

JA910583Y